Published in final edited form as:
Neurosci Res. 2012 April ; 72(4): 296–305. doi:10.1016/j.neures.2012.01.007.

Severe Vestibular Dysfunction and Altered Vestibular Innervation in Mice Lacking Prosaposin

Omar Akil, PhD and
Department of Otolaryngology- Head & Neck Surgery, University of California San Francisco, San Francisco, CA, 94143-0449. Phone: (01) 415-476-0728. oakil@ohns.ucsf.edu

Lawrence R. Lustig, MD
Department of Otolaryngology-Head & Neck Surgery, University of California San Francisco, 533 Parnassus Avenue Room U401, San Francisco, CA 94143-0449, llustig@ohns.ucsf.edu, Phone: (01) 415-476-0728, Fax: (01) 415-476-0708

Abstract

Prosaposin, a precursor of four glycoprotein activators (Saposin A, B, C and D) for lysosomal hydrolases, has previously been shown to be important for normal adult cochlear innervation and the maintenance of normal hearing. In these studies, we now investigate prosaposin in normal vestibular epithelium and the functional impairment of balance caused by prosaposin ablation.

In normal mice, prosaposin is localized to all 3 vestibular end-organs (ampullae, saccule, and utricle) and Scarpa's ganglion by RT-PCR, Western blot analysis and immunofluorescence. Ablation of prosaposin function caused severe vestibular dysfunction on a battery of behavioral tasks. Histologically, the KO mice demonstrated an exuberant cellular proliferation below the vestibular hair cells with disruption of the supporting cells. Electron microscopy further demonstrated inclusion bodies and cellular proliferation disturbing the normal neuroepithelial structure of the vestibular end-organs. Lastly, immunofluorescence (neurofilament 200 and synaptophysin) staining suggests that this cellular proliferation corresponds to afferent and efferent neuronal overgrowth. These data suggest that prosaposin plays a role not only in the maintenance of normal hearing but also an important role in the neuronal maturation processes of the vestibular sensory epithelium and the maintenance of normal vestibular system function.

Keywords

Prosaposin; Vestibular sensory epithelium; Balance; Efferent and Afferent nerves; Vestibular supporting cells

1. Introduction

Prosaposin is a multifunctional protein with both intra- and extra-cellular functions. Intracellularly, prosaposin (65–70KDa) is proteolytically cleaved within lysosomes into four 10–15KDa polypeptides termed saposins (A, B, C and D), that are necessary for the activity

Correspondence to: Lawrence R. Lustig.

of specific lysosomal glycosphingolipid (GSL) hydrolases (Sun et al., 2002). The physiological importance of this protein has been demonstrated by the genetic deficiencies of individual saposins or prosaposin that lead to various GSL-related disorders such as Gaucher disease (Holtschmidt et al., 1991; Paton et al., 1992; Rafi et al., 1993; Hulkova et al., 2001). Extracellularly, intact prosaposin shows *ex vivo* and *in vivo* function as a neurite outgrowth or nerve regeneration factor, respectively (O'Brien et al., 1994; O'Brien et al., 1995; Kotani et al., 1996; Qi et al., 1996). The sequence of prosaposin involved in neurite outgrowth has been localized to 21 amino acids in the amino-terminal half of saposin C (O'Brien et al., 1995; Qi et al., 1996).

Studies on prosaposin within the ear have been limited. Terashita et al ((Terashita et al., 2007) demonstrated localization of prosaposin within the rat cochlea. Akil *et al* (Akil et al., 2006) demonstrated that prosaposin knockout (KO) mice develop a progressive hearing loss beginning at P19, with an abnormal proliferation of afferent and efferent neurons as a likely causative factor in this loss of hearing. These studies strongly suggest that normal prosaposin function is required for maintenance of adult cochlear innervations patterns and consequently the maintenance of normal hearing (Akil et al., 2006).

During these initial studies on prosaposin in the cochlea, it was noted that the prosaposin KO mice demonstrated behaviors consistent with vestibular dysfunction, including circling, an unsteady gait, and difficulties in maintaining balance, suggesting that in addition to its role in hearing, prosaposin also contributes to the vestibular function as well. The vestibular system consists of the semicircular canals (ampulla), which detect changes in the angular acceleration, and the utricle and the saccule, which detect changes in the linear acceleration and head position with respect to gravity (Walls, 1962; Land, 1999; Spoor et al., 2002). In these studies, we now investigate prosaposin in normal vestibular epithelium and the effect of prosaposin ablation on balance. Similar to what is seen in the organ of Corti, the absence of prosaposin in the KO mice causes profound vestibular end organ defects demonstrated by a marked cellular proliferation and vestibular supporting cell disruption. Taken together these results indicate that prosaposin plays an important role in the neuronal maturation processes of the vestibular sensory epithelium and the maintenance of normal vestibular system function.

2. Material and Methods

2.1. Animals

FVB wild mice were purchased from Charles River and FVB prosaposin knockout mice were generously provided by Dr. Greg Grabowski, University of Cincinnati, Cincinnati, OH). The general and central nervous system phenotype of this mouse has been previously described (Ninkina et al., 2003). All procedures and animal handling were done according to national ethic guidelines, approved and complied with all protocol requirements at the University of California, San Francisco Institutional Animal Care and Use Committee (IACUC).

2.2. Reverse-transcriptase Polymerase Chain Reaction (RT-PCR)

The total RNA harvested from mice vestibular epithelium (ampulla, saccule, utricle and Scarpa's ganglia) extractions was reverse transcribed with superscript II RNase H^- (Invitrogen) for 50min at 42°C, using oligodT primers. 2μl of RT reaction product were used for subsequent PCR (Taq DNA Polymerase, Invitrogen) of 35 cycles using the following parameters: 94°C for 30sec, 60°C for 45sec, 72°C for 1 minute, followed by a final extension of 72°C for 10 minutes and storage at 4°C. Primers were designed to amplify a unique sequence of mouse prosaposin. The PCR primers that were used (GenBank ID:

NM_011179) are: forward -gcaccaaggaggaaatcctggcc- reverse - ggaacccccttttgcccttcccc- and were designed to amplify a 400bp fragment spanning two introns (Zhao et al., 1997). Controls (-RT) included vestibular mRNA from each vestibular epithelium end organ without reverse transcriptase.

Analysis of each PCR sample was then performed on 2% agarose gels containing 0.5 μg/ml ethidium bromide. Gels were visualized using a digital Camera and image processing system (Kodak, Rochester NY). Candidate bands were cut out and the DNA was extracted (Qiaquick gel extraction kit, Qiagen) and sequenced (Elim Biopharmaceuticals, Inc. Hayward, CA). The PCR product was then compared directly to the full mouse prosaposin sequence for identity.

2.3. Immunofluorescence

Prosaposin wild and KO mice were anesthetized and their cochleae were isolated, dissected, perfused through the oval and round windows by 2% paraformaldehyde in 0.1M phosphate buffer (PB) at pH 7.4 and incubated in the same fixative for 2 hours. After fixation cochleae were rinsed with PB and immersed in 5% EDTA in 0.1M PB for decalcification. When cochleae were totally decalcified (2–3 days), they were incubated overnight in 30% sucrose for cryoprotection. The cochleae then were embedded in O.C.T. Tissue Tek Compound (Miles Scientific). Tissues were cryosectioned parallel to the modiolus at 10–12 μm thickness for immunofluorescence, mounted on Superfrost™ microscope slides (Erie Scientific, Portsmouth NH) and stored at −20°C until use.

For immunofluorescent staining of the wild and KO vestibular epithelium sections, a rabbit polyclonal prosaposin antibody was made toward the C-terminal end of mouse prosaposin, corresponding to saposin D (generously provided by Dr. Greg Grabowski, University of Cincinnati, Cincinnati, OH) (Akil et al., 2006), a rabbit polyclonal neurofilament-200 antibody (NF-200; Chemicon, Temecula, CA), which labels afferent and efferent auditory fibers (Berglund and Ryugo, 1991), or a rabbit polyclonal synaptophysin antibody (Zymed, South San Francisco, CA), which labels efferent auditory fibers (Schimmang et al., 2003) were used in this study. After incubation at 37°C for 30 min, the sections were rinsed twice for 5 min in 0.1 M PBS, pH7.4, and then preincubated for 1 h in the blocking buffer: 0.25% Triton X-100 and 5% normal goat serum (NGS) (for prosaposin), 0.25% Triton X100 and 30% NGS (for NF-200), or 10% NGS without Triton X100 (for synaptophysin). The sections were then incubated in a humid chamber overnight at 4°C with the primary antibodies: 1:300 prosaposin or 1/500 NF-200 diluted in the blocking buffer or 1/200 synaptophysin diluted in PBS. The slides were then rinsed (2× for 10 min) and incubated for 2 hours in goat anti-rabbit IgG conjugated to Cy3 diluted to 1:4000. The sections were rinsed in PBS (2× for 10 min) and mounted in equal parts glycerol/PBS and cover-slipped. Slides treated with the same technique but without incubation in the primary antibody were used as a control. In all experiments, fluorescent dye 4, 6-diamidino-2-phenylindole (DAPI 1.5 μg/ml in PBS, Sigma) was used to counterstain nuclei. Following the removal of the secondary antibodies and prior to the final washes, the sections were exposed for 15 min at room temperature to DAPI staining which allowed visualization of the nuclei together with immunofluorescence. Then the slides were observed with an Olympus microscope with confocal immunofluorescence.

2.4. Western blot analysis

The FVB wild mice were anesthetized quickly decapitated and all tissues, including brain (control), ampulla, saccule, and utricle, were dissected in ice-cold phosphate-buffered saline (PBS). Each tissue was homogenized separately in a lysis buffer containing (20mM Tris HCl pH 7.5–8, 150mM NaCl, 0.5% sodium deoxycolate, 1% Triton X100, 0.1 SDS, 1mM

EDTA, 1 mM PMSF, and protease inhibitor cocktail) with a disposable pestle in a sterile Eppendorf tube. The tubes were sealed and samples were boiled at 95°C for 5 minutes and then frozen in crushed dry ice. Specimens were next thawed at 37°C for 1 minute and kept on ice. The homogenate was spun 10 min at 14,000 RPM at 4°C and the protein concentration in the supernatant was determined by Bradford assay. Sample buffer was added to approximately 100μg of the supernatant of each sample, boiled at 97°C for 5 minutes, separated by SDS-PAGE on a 4–20% gradient acrylamide gel and transferred to nitrocellulose membrane (Luebke et al., 2005). The blot was incubated for 1 hour in blocking buffer containing 5% nonfat dry milk in PBS-T (phosphate buffer saline + 0.1% Tween 20) and then incubated overnight at 4°C with rabbit anti mouse prosaposin antibody (used for immunohistochemistry) diluted in 1%BSA in PBS-T (prosaposin antibody 1/500). The membrane was washed in PBS-T and incubated for 2 hours at room temperature with the secondary antibody (donkey anti-rabbit IgG peroxidase conjugate GE Healthcare cat# NA934) 1/3000. The blot was washed again with PBS-T dried and then incubated for 1min with the chemiluminescence reagent NEL 103 (Perkin Elmer). After one minute the membrane was dried and exposed to KODAK X_OMAT blue film. Then the films were developed for protein visualization.

2.5. Histology

2.5.1. Light microscopy—Prosaposin knock-out mice and wild littermates (~P25) were anesthetized and their cochleae were isolated, dissected, perfused through the round and oval windows with a solution of 2% paraformaldehyde and 2% glutaraldehyde in 0.1 M phosphate buffered solution, pH 7.4, and then incubated in the same fixative overnight at 4°C. The cochleae were rinsed with 0.1 M PB and post fixed in 1% osmium tetroxide for 2 hours. The cochlea subsequently immersed in 5% EDTA. The decalcified cochleae were dehydrated in ethanol and propylene oxide and embedded in Araldite 502 resin (Electron Microscopy Sciences, Fort Washington, PA) and sectioned at 5 μm thickness parallel to the cochlea modiolus. Then sections were stained with Toluidine Blue and mounted with Permount (Fisher Scientific, Houston, TX) on microscope slides and visualized with a Leica microscope.

2.5.2. Electron microscopy—The Cochlea of 25 day-old mice was surgically exposed, a stapedectomy was performed, and the round window perforated. Temporal bones were preserved by gentle *in vivo* perfusion of fixative (1.5% glutaraldehyde and 2.5% paraformaldehyde, buffered to pH 7.4, with 0.1M phosphate) through the perilymphatic channels, followed by post-fixation with a solution of 1% osmium tetroxide and 1.5% potassium ferricyanide phosphate buffered solution (potassium ferricyanide was used to improve contrast). The vestibular epithelium was dissected, osmicated, dehydrated, and then embedded in Epon. Thick sections (1μm) were mounted onto glass slides and counterstained with toluidine blue. Once the vestibular epithelium hair cells were observed, several ultrathin silver to gray sections were collected on Formvar films on slotted grids, stained with saturated aqueous 2% uranyl acetate and 0.4% lead citrate in 0.15N sodium hydroxide. The stained sections then examined at 60 kV in a JEOL-JEM 100S transmission electron microscope.

2.6. Vestibular system function

Vestibular function was assessed with four commonly employed tests including the air righting reflex, contact righting reflex, swimming test, and circling/rearing frequency (Khan et al., 2004). *The air righting reflex* (Ossenkopp et al., 1990) examines the ability of the mice to right themselves in the air. In brief, mice were held in a supine position and dropped onto a soft padded surface from a height of 50 cm. The average percentage of trials each mouse landed on all four feet was determined from five attempts for each mouse. *The*

contact righting reflex test (Ossenkopp et al., 1990; Khan et al., 2004) examines the ability of the mice to right themselves when placed supine on a horizontal surface. Mice were put in a 60 ml opaque plastic syringe so that they could roll over but could not turn around or rear. The syringe was inverted until the animal was in the supine position, and the average time for the mice to return to the upright position within the syringe was determined for three trials for each mouse. *The swimming test* (Lim et al., 1978; Sawada et al., 1994; Ornitz et al., 1998; Jones et al., 1999; Khan et al., 2004), was performed on each animal. Mice were put in a 20×40 cm Plexiglas cage filled with water at room temperature for 60 sec. The average swimming time with the head above water was determined for three trials for each mouse. Finally *the circling and rearing frequency* tests (Ossenkopp et al., 1990) quantitate the number of rears or circles occurring in 1 min, and was assessed every 10 min for an hour and used as an estimate of hourly frequency. Statistical analyses were performed using unpaired Student's t-test, with significance defined as $p < 0.05$.

2.7. Acoustic Brainstem Response Testing

Auditory brainstem response (ABR) was performed as previously described (Akil et al., 2006) with prosaposin knockout (KO) mice, heterozygote (Het) and wild-type (WT) littermates ~P25. Briefly, all auditory testing was performed in a sound-proof chamber. Before acoustic testing, mice were anesthetized by intraperitoneal injection of a mixture of Ketamine hydrochloride (Ketaset, 100 mg/ml) and xylazine hydrochloride (xyla-ject, 10 mg/ml) and boosted with one fifth the original dose as required. Body temperature was maintained with a heating pad and monitored with a rectal probe throughout recording.

The evoked acoustic brainstem response thresholds were differentially recorded from the scalp of knock-out mice at age ~P25. Responses were recorded using subdermal needle electrodes at the vertex, below the pinna of the left ear (reference), and below the contralateral ear (ground). The sound stimuli used included clicks (5ms duration; 31Hz) and tone pips at 8, 16, and 32 kHz (10ms duration; cos2 shaping; 21Hz). Measurements were done using the TDT BioSig III system (Tucker Davis Technologies). For each stimulus, electroencephalographic (EEG) activity was recorded for 20 ms at a sampling rate of 25KHz, filtered (0.3–3KHz), and waveforms from 512 stimuli were averaged for click responses, and 1000 stimuli for frequency specific stimuli (8, 16 and 32 KHz). ABR waveforms were recorded in 5 dB sound pressure level (SPL) intervals down from the maximum amplitude. Threshold was defined as the lowest stimulus level at which response peaks for waves I–V were clearly and repeatably present upon visual inspection. These threshold judgments were confirmed by analysis of stored waveforms. Data were obtained from the prosaposin KO (n=6) and wild type (n=6) mice littermates.

Comparison of each group of animals (KO vs. wild-type) was performed using 1 way ANOVA with Bonferroni post-hoc testing. Significance was defined at $p < 0.05$.

3. Results

3.1. Prosaposin localization in normal postnatal vestibular epithelium

Several methods were used to detect and localize prosaposin within the normal rodent vestibular end-organs (Figure 1–2). RT-PCR analysis was initially performed to study mRNA expression in the mice vestibular epithelium. As shown (Figure 1A), prosaposin mRNA was detected in P25 mouse ampullae, saccule, utricle and Scarpa's ganglia. As predicted from our previous studies (Akil et al., 2006), expression was also seen within the organ of Corti. These results are also consistent with prior studies demonstrating widespread prosaposin expression throughout the body in a number of cell types (Morales et al., 1996).

To demonstrate the presence of translated prosaposin protein within the vestibular epithelium, western blot analysis was performed. On western blot testing, an antibody against the saposin D domain labeled a band between 65–70 KDa in whole mouse vestibular end organs (Figure 1B) in addition to labeling of extracted protein from the brain (positive control) and weaker bands for microdissected ampulla, saccule and utricle.

Lastly, immunohistology was used to characterize the expression of prosaposin within the vestibular end organs using a rabbit polyclonal antibody directed against the C-terminal end of prosaposin, corresponding to saposin D (Figure 2). (Immunofluorescence labeling thus does not differentiate between prosaposin, an active protein itself, and one of its cleaved product saposin D). In these specimens, staining appeared as an intense punctate label in the cytoplasm of the Scarpa's ganglion neurons and around the nucleus of the vestibular hair cells of the ampulla and utricle. Saccular hair were weakly immunoreactive and no labeling was identified within the supporting cells (Figure 2).

3.2. Vestibular Phenotype of the Prosaposin Knockout Mouse

Prosaposin KO mice displayed a number of features consistent with vestibular dysfunction. At P25, mice frequently circled, more commonly in a counter-clockwise direction (Figure 3A) and had extreme difficulty maintaining balance and gait when walking or standing (Figures 3B–D).

To more quantitatively assess vestibular function, a number of tests were administered to the mice (Figure 4). On the *circling frequency test* (Figure 4A) (Ossenkopp et al., 1990), which quantifies the number of circles occurring in 1 min, and assessed every 10 min for an hour for an estimate of hourly frequency, WT mice had essentially no circling tendencies, while the KO mice circled, predominantly to the left, though occasionally to the right. For *contact righting reflex testing* (Ossenkopp et al., 1990; Khan et al., 2004), wild-type mice recognized their upside down position and righted themselves inside the syringe on average within 10 seconds while it took the KO mice 27 seconds on average to recognize that they were upside down, and they further made little or no effort to right themselves (Figure 4B). This difference was statistically significant ($p=0.039$). For air *righting reflex testing* (Ossenkopp et al., 1990), when dropped supine from a height of 50 cm, wild-type mice righted themselves in mid-air, landing on their feet 100% of the time (Figure 4C). In contrast, the prosaposin KO mice landed on their back or side 90% of the time. This difference was statistically significant ($p<0.01$). Lastly, in the *swim test*, measuring the ability to orient in a head-up position and swim comfortably for a full 60 seconds (Sawada et al., 1994), all WT mice exhibited normal swimming (Figure 4D). In contrast, not one KO mouse was able to swim or orient properly in water. The mice were unable to keep their heads above water for more than 15 seconds, and consistently had to be rescued to prevent drowning. The difference between these groups was statistically significant ($p=0.03$). Together, these 4 tests demonstrate severe functional deficits of the vestibular system in the prosaposin KO mice.

3.3. Histologic changes in the Prosaposin Knockout Mouse

Standard histological analysis (Figure 5) was assessed to gain a better understanding of the effects of the prosaposin null mutation on the vestibular end-organs. In contrast to wild-type littermates, KO mice revealed severe structural abnormalities in the ampullae, saccule and utricle (Figure 5). Most notably, this was a marked cellular proliferation below the vestibular hair cells causing disruption of the supporting cells. Further, some of the afferent neurons entering the neuroepithelium demonstrate swelling below the hair cells whereas Scarpa's ganglion is normal in appearance (data not shown).

At the ultramicroscopic level, these changes appear even more striking (Figure 6). As compared to wild-type ampullae (Figure 6A), the KO mice ampullae (Figure 6B,D,E F) and saccule (figure 6C) demonstrate marked cellular hypertrophy with what appear to be fatty deposits at the base of the vestibular hair cells of the ampulla, saccule and utricle resulting in disruption of the supporting cells of the vestibular end organs. As seen in light microscopy, some of the afferents entering the epithelium also demonstrate swelling below the hair cells.

To further evaluate these proliferative changes seen below the hair cells, immunoflouorescence with antibodies against synaptophysin, an efferent auditory fiber label (Schimmang 2003), and NF-200, an afferent and efferent neuronal label (Berglund and Ryugo, 1991), were employed (Figure 7). Histological sections were analyzed in P25 mice, a time-point at which KO mice consistently demonstrate circling, unsteady gait, and difficulties in maintaining balance. In contrast to the normal staining pattern seen in the wild-type mice, the KO mice demonstrate an intense NF-200 staining pattern in the region corresponding to the cellular proliferation in the base of the vestibular hair cells of the ampulla (Amp), saccule (Sac) and utricle (Utr), disrupting the vestibular hair cells and supporting cells. Synaptophysin shows a nearly identical staining pattern as NF-200, indicating that the hyper-cellular region in the base of the vestibular hair cells consists of abnormal afferent and efferent neuronal terminals in the KO mice.

3.4. Functional analysis of hearing in KO mice

Hearing in the KO mice was tested using standard ABR threshold analysis to verify the hearing loss phenotype, as was previously shown (Akil et al., 2006). Mice were bred in an FVB background, a strain with minimal auditory deficits. Mice at P25 were thus tested using the sound stimulus: broadband click and pure tones of 8, 16, and 32 kHz. As shown in Figure 8A (Figures 8 A presents only click stimulus), the Prosaposin KO mice exhibited statistically significantly elevated ABR thresholds (~70–80dB) for each of the four sound stimuli, when compared with the threshold (28–48dB) for the wild and heterozygotes littermates, results expected based on prior studies (Akil et al., 2006).

4. Discussion

The objectives of this study were two-fold; first to characterize prosaposin within the normal vestibular system and second, to assess the consequences on balance when prosaposin function is ablated.

Although previous reports have indicated that prosaposin protein exhibits ubiquitous expression (Morales et al., 1996), there is no information about the expression of prosaposin in the vestibular system. Prior reports have only localized prosaposin to the cochlea within the temporal bone (Akil et al., 2006; Terashita et al., 2007). In the current study we demonstrate prosaposin mRNA expression in the vestibular end organs and Scarpa's ganglion using RT-PCR (figure 1A), and localized protein expression using Western blot and immunofluorescence (figures 1B and 2) within the ampulla, saccule and utricle.

Mutant mice with inherited vestibular system dysfunction and normal mice in which vestibular system has been experimentally damaged exhibit typical functional patterns, including circling, unsteady gait and difficulties in maintaining balance (Figure 3) (Hunt et al., 1987; Ossenkopp et al., 1990; Doolittle et al., 1996; Llorens and Rodriguez-Farre, 1997; Khan et al., 2004). These behaviors were similar to those seen in the prosaposin KO mice, indicating that ablation of prosaposin function caused a severe vestibular deficit. The severe phenotype consisting of neuronal cellular proliferation and fatty deposits in the vestibular end-organs strongly suggests that the changes seen are responsible for these abnormal behaviors. It should be noted that prior studies have also demonstrated that prosaposin KO

mice exhibit a number of abnormalities within the central nervous system, including the cerebellum, with similar pathologic changes that were seen in the inner ear. These include an inclusion body accumulation with leukodystrophy and glycosphingolipid accumulation (Fujita et al., 1996; Sun et al., 2002). Thus, we cannot definitely rule-out central pathology as a cause or contributor to the balance dysfunction observed in the KO mice. Future studies, including vestibular-ocular reflex testing and/or caloric response measures could potentially resolve the question of whether the balance abnormalities observed are peripherally- vs. centrally-mediated in this mouse model.

The vestibular system consists of the semicircular canals, which detect changes in angular acceleration, and the utricle and the saccule, which detect changes in the linear acceleration and head position with respect to gravity, respectively. Histological analyses of the prosaposin KO vestibular epithelium, at both the light and ultrastructural levels, demonstrate a severe defect in all the end-organs (Figures 5–6). The source of the aberrant hypertrophy of vestibular afferent and efferent fibers in the prosaposin KO mice, similar to what was previously seen in the auditory system (Akil et al., 2006), as evidenced by the synaptophysin and NF200 staining (figure 7) may be a result of failed neuronal path-finding or innervation that would be normally supported by prosaposin or one of its cleaved products saposin A–D. This suggests that feedback signals that normally terminate vestibular afferent and efferent outgrowth fail in prosaposin KO mice. This is thought to be caused by the perturbation of the supporting cells regulating synapse formation in the vestibular epithelium as demonstrated by Gomez-Casati et al., 2010, where they found that the vestibular supporting cells contribute in vivo to vestibular synapse formation and that this is mediated by reciprocal signals between sensory neurons and supporting cells. Less likely, centrally mediated changes may also explain some of these findings, due to reduced or desynchronized neuronal activity from the central neuronal demyelination and degeneration that has also been described in the prosaposin KO mouse (Fujita et al., 1996; Oya et al., 1998; Sun et al., 2002).

The cellular proliferation seen beneath the vestibular hair cells in the end-organs appear to be swollen neurons entering the neuroepithelium (Figures 5 and 6). Since these regions are strongly labeled by antibodies to both synaptophysin and NF200, this suggests that this cellular proliferation corresponds to afferent and efferent neurite overgrowth (Figure7), similar to that seen in the organ of Corti (Akil et al., 2006). Taken together these results demonstrate that prosaposin or one of its cleaved products, saposin A–D plays an important role in the normal maturation and function of the vestibular end organs. Alternatively, it is possibly that the vestibular neurons develop normally but subsequently degenerate due to some unknown effect of prosaposin.

Prosaposin knockout mice were significantly deficient in all four of the vestibular functional tests studied (Figure 4), and provide clear evidence for vestibular dysfunction. The prosaposin KO mice exhibited loss of the air-righting and contact righting reflexes.

In conclusion, as in the organ of Corti, prosaposin is found throughout the vestibular end-organs, and appears to play an important role in the neuronal maturation processes of the vestibular sensory epithelium and the maintenance of normal vestibular system function.

- Prosaposin is expressed and localized in vestibular end-organs and Scarpa’s ganglia
- Prosaposin is important for the maintenance of normal vestibular system function
- Prosaposin ablation leads to severe behavioral vestibular dysfunction

- Prosaposin plays an important role for neuronal maturation of the vestibular organs

Acknowledgments

We would like to acknowledge the support of Hearing Research Inc and Dr. Bernard Kramer for funding for these studies and Dr. Greg Grabowski, University of Cincinnati for generously providing us with the prosaposin knock-out mice. In addition, we recognize the support from the NIH NIDCD K08 DC00189 for supporting initial studies leading up to this work.

References

Akil O, Chang J, Hiel H, Kong JH, Yi E, Glowatzki E, Lustig LR. Progressive deafness and altered cochlear innervation in knock-out mice lacking prosaposin. J Neurosci. 2006; 26:13076–13088. [PubMed: 17167097]

Berglund AM, Ryugo DK. Neurofilament antibodies and spiral ganglion neurons of the mammalian cochlea. J Comp Neurol. 1991; 306:393–408. [PubMed: 1865000]

Doolittle, D.; Davisson, M.; Guidi, J.; MC, G. Catalog of mutant genes and polymorphic loci. In: Lyon, F.; Rastan, S.; Brown, S., editors. Genetic variants and strains of the laboratory mouse. Oxford: Oxford University Press; 1996. p. 17-854.

Fujita N, Suzuki K, Vanier MT, Popko B, Maeda N, Klein A, Henseler M, Sandhoff K, Nakayasu H, Suzuki K. Targeted disruption of the mouse sphingolipid activator protein gene: a complex phenotype, including severe leukodystrophy and wide-spread storage of multiple sphingolipids. Hum Mol Genet. 1996; 5:711–725. [PubMed: 8776585]

Holtschmidt H, Sandhoff K, Kwon HY, Harzer K, Nakano T, Suzuki K. Sulfatide activator protein. Alternative splicing that generates three mRNAs and a newly found mutation responsible for a clinical disease. J Biol Chem. 1991; 266:7556–7560. [PubMed: 2019586]

Hulkova H, Cervenkova M, Ledvinova J, Tochackova M, Hrebicek M, Poupetova H, Befekadu A, Berna L, Paton BC, Harzer K, Boor A, Smid F, Elleder M. A novel mutation in the coding region of the prosaposin gene leads to a complete deficiency of prosaposin and saposins, and is associated with a complex sphingolipidosis dominated by lactosylceramide accumulation. Hum Mol Genet. 2001; 10:927–940. [PubMed: 11309366]

Hunt MA, Miller SW, Nielson HC, Horn KM. Intratympanic injection of sodium arsanilate (atoxyl) solution results in postural changes consistent with changes described for labyrinthectomized rats. Behav Neurosci. 1987; 101:427–428. [PubMed: 3606813]

Jones SM, Erway LC, Bergstrom RA, Schimenti JC, Jones TA. Vestibular responses to linear acceleration are absent in otoconia-deficient C57BL/6JEi-het mice. Hear Res. 1999; 135:56–60. [PubMed: 10491954]

Khan Z, Carey J, Park HJ, Lehar M, Lasker D, Jinnah HA. Abnormal motor behavior and vestibular dysfunction in the stargazer mouse mutant. Neuroscience. 2004; 127:785–796. [PubMed: 15283975]

Kotani Y, Matsuda S, Sakanaka M, Kondoh K, Ueno S, Sano A. Prosaposin facilitates sciatic nerve regeneration in vivo. J Neurochem. 1996; 66:2019–2025. [PubMed: 8780031]

Land MF. Motion and vision: why animals move their eyes. J Comp Physiol A. 1999; 185:341–352. [PubMed: 10555268]

Lim, D.; Erwy, L.; Clark, D. Tilted- head mice with genetic otoconial anomaly. Behavioral and morphological correlates. In: Hood, D., editor. Vestibular Mechanisms in Health and Disease. London: Academic press; 1978. p. 195-206.

Llorens J, Rodriguez-Farre E. Comparison of behavioral, vestibular, and axonal effects of subchronic IDPN in the rat. Neurotoxicol Teratol. 1997; 19:117–127. [PubMed: 9136128]

Luebke AE, Maroni PD, Guth SM, Lysakowski A. Alph-9 nicotinic acetylcholine receptor immunoreactivity in the rodent vestibular labyrinth. J Comp Neurol. 2005; 492:323–333. [PubMed: 16217793]

Morales CR, El-Alfy M, Zhao Q, Igdoura SA. Expression and tissue distribution of rat sulfated glycoprotein-1 (prosaposin). J Histochem Cytochem. 1996; 44:327–337. [PubMed: 8601692]

Ninkina N, Papachroni K, Robertson DC, Schmidt O, Delaney L, O'Neill F, Court F, Rosenthal A, Fleetwood-Walker SM, Davies AM, Buchman VL. Neurons expressing the highest levels of gamma-synuclein are unaffected by targeted inactivation of the gene. Mol Cell Biol. 2003; 23:8233–8245. [PubMed: 14585981]

O'Brien JS, Carson GS, Seo HC, Hiraiwa M, Kishimoto Y. Identification of prosaposin as a neurotrophic factor. Proc Natl Acad Sci U S A. 1994; 91:9593–9596. [PubMed: 7937812]

O'Brien JS, Carson GS, Seo HC, Hiraiwa M, Weiler S, Tomich JM, Barranger JA, Kahn M, Azuma N, Kishimoto Y. Identification of the neurotrophic factor sequence of prosaposin. Faseb J. 1995; 9:681–685. [PubMed: 7768361]

Ornitz DM, Bohne BA, Thalmann I, Harding GW, Thalmann R. Otoconial agenesis in tilted mutant mice. Hear Res. 1998; 122:60–70. [PubMed: 9714575]

Ossenkopp KP, Prkacin A, Hargreaves EL. Sodium arsanilate-induced vestibular dysfunction in rats: effects on open-field behavior and spontaneous activity in the automated digiscan monitoring system. Pharmacol Biochem Behav. 1990; 36:875–881. [PubMed: 2217517]

Oya Y, Nakayasu H, Fujita N, Suzuki K, Suzuki K. Pathological study of mice with total deficiency of sphingolipid activator proteins (SAP knockout mice). Acta Neuropathol. 1998; 96:29–40. [PubMed: 9678511]

Paton BC, Schmid B, Kustermann-Kuhn B, Poulos A, Harzer K. Additional biochemical findings in a patient and fetal sibling with a genetic defect in the sphingolipid activator protein (SAP) precursor, prosaposin. Evidence for a deficiency in SAP-1 and for a normal lysosomal neuraminidase. Biochem J. 1992; 285((Pt 2)):481–488. [PubMed: 1637339]

Qi X, Qin W, Sun Y, Kondoh K, Grabowski GA. Functional organization of saposin C. Definition of the neurotrophic and acid beta-glucosidase activation regions. J Biol Chem. 1996; 271:6874–6880. [PubMed: 8636113]

Rafi MA, de Gala G, Zhang XL, Wenger DA. Mutational analysis in a patient with a variant form of Gaucher disease caused by SAP-2 deficiency. Somat Cell Mol Genet. 1993; 19:1–7. [PubMed: 8460394]

Sawada I, Kitahara M, Yazawa Y. Swimming test for evaluating vestibular function in guinea pigs. Acta Otolaryngol. 1994; 510 Suppl:20–23.

Schimmang T, Tan J, Muller M, Zimmermann U, Rohbock K, Kopschall I, Limberger A, Minichiello L, Knipper M. Lack of Bdnf and TrkB signalling in the postnatal cochlea leads to a spatial reshaping of innervation along the tonotopic axis and hearing loss. Development. 2003; 130:4741–4750. [PubMed: 12925599]

Spoor F, Bajpai S, Hussain ST, Kumar K, Thewissen JG. Vestibular evidence for the evolution of aquatic behaviour in early cetaceans. Nature. 2002; 417:163–166. [PubMed: 12000957]

Sun Y, Qi X, Witte DP, Ponce E, Kondoh K, Quinn B, Grabowski GA. Prosaposin: threshold rescue and analysis of the "neuritogenic" region in transgenic mice. Mol Genet Metab. 2002; 76:271–286. [PubMed: 12208132]

Terashita T, Saito S, Miyawaki K, Hyodo M, Kobayashi N, Shimokawa T, Saito K, Matsuda S, Gyo K. Localization of prosaposin in rat cochlea. Neurosci Res. 2007; 57:372–378. [PubMed: 17156877]

Walls G. The evolutionary history of eye movements. Vision Research. 1962; 2:69–80.

Zhao Q, Hay N, Morales CR. Structural analysis of the mouse prosaposin (SGP-1) gene reveals the presence of an exon that is alternatively spliced in transcribed mRNAs. Mol Reprod Dev. 1997; 48:1–8. [PubMed: 9266755]

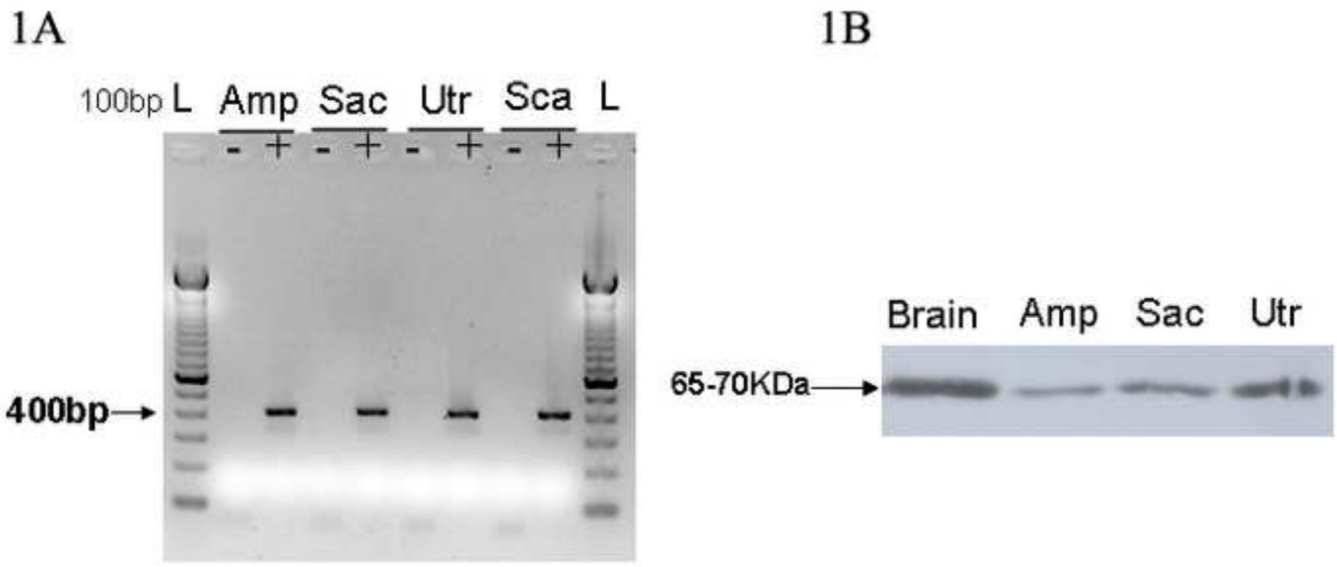

Figure 1.

Localization of Prosaposin in the rodent vestibular system using RT-PCR (1A) and Western blot (1B) from microdissected mice vestibular tissue. 1A- Microdissected mice vestibular tissues including Ampulla (**Amp**), Saccule (**Sac**), Utricle (**Utr**) and Scarpa's ganglia (**Sca**) were used to detect the presence of prosaposin mRNA. The gel above demonstrates the presence of prosaposin mRNA in all vestibular end organs and the Scarpa's ganglia with an expected band size of 400bp. Controls lacking reverse-transcriptase (non RT denoted with a '-') are included and show no amplification. 1B-Western blot was used to assess for the presence of prosaposin protein in the vestibular system and the brain tissues. In lane 1, mouse brain served as a positive control. Lanes 2 (Ampulla), 3 (Saccule) and 4 (Utricle) show that prosaposin is found in all mice vestibular end-organs though less than the expression in the brain as demonstrated by the band at ~65–70kDa.

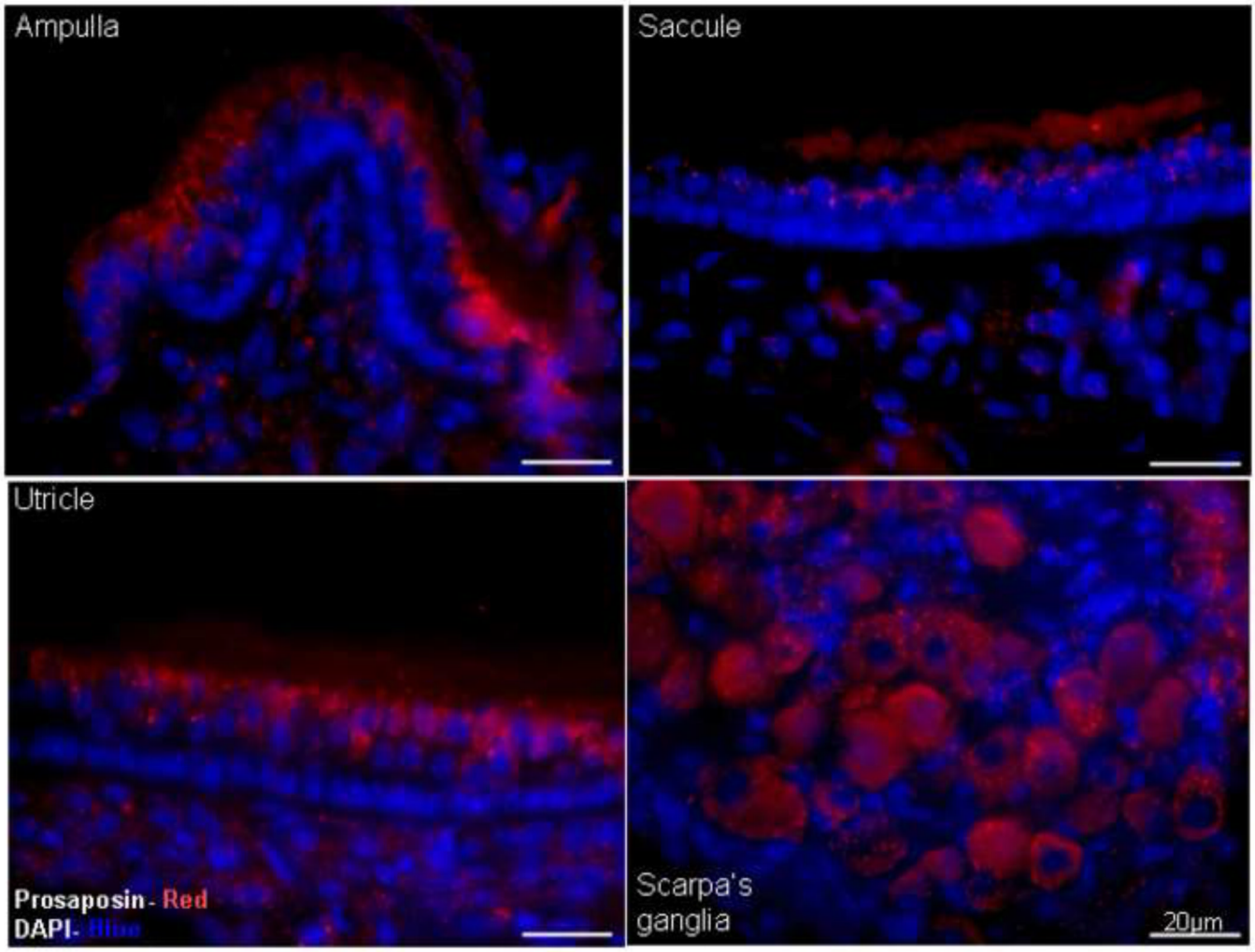

Figure 2.
Immunofluorescence using an antibody against prosaposin demonstrates that prosaposin (Red) is predominantly localized around the vestibular hair cells of the ampulla, saccule and utricle and the cell bodies of the Scarpa's ganglia. DAPI staining (Blue) was used to counterstain nuclei. Scale bars: 20µm.

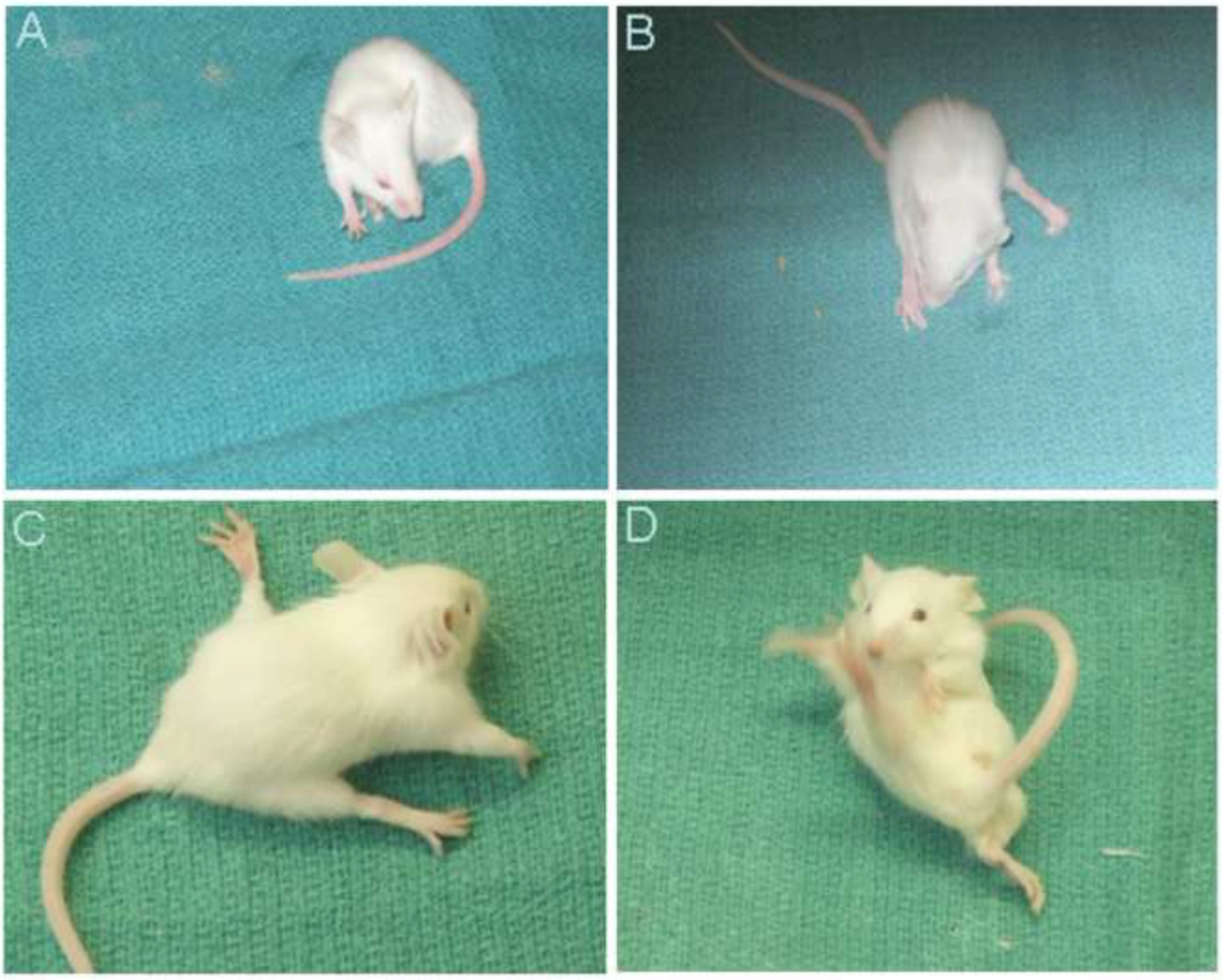

Figure 3.
Phenotype of the Prosaposin KO mice at P25 exhibiting an unsteady gait and difficulty in maintaining balance. Picture A- Circling of the prosaposin KO mouse and pictures B to D show unsteady gait and dysequilibrium in the KO mouse.

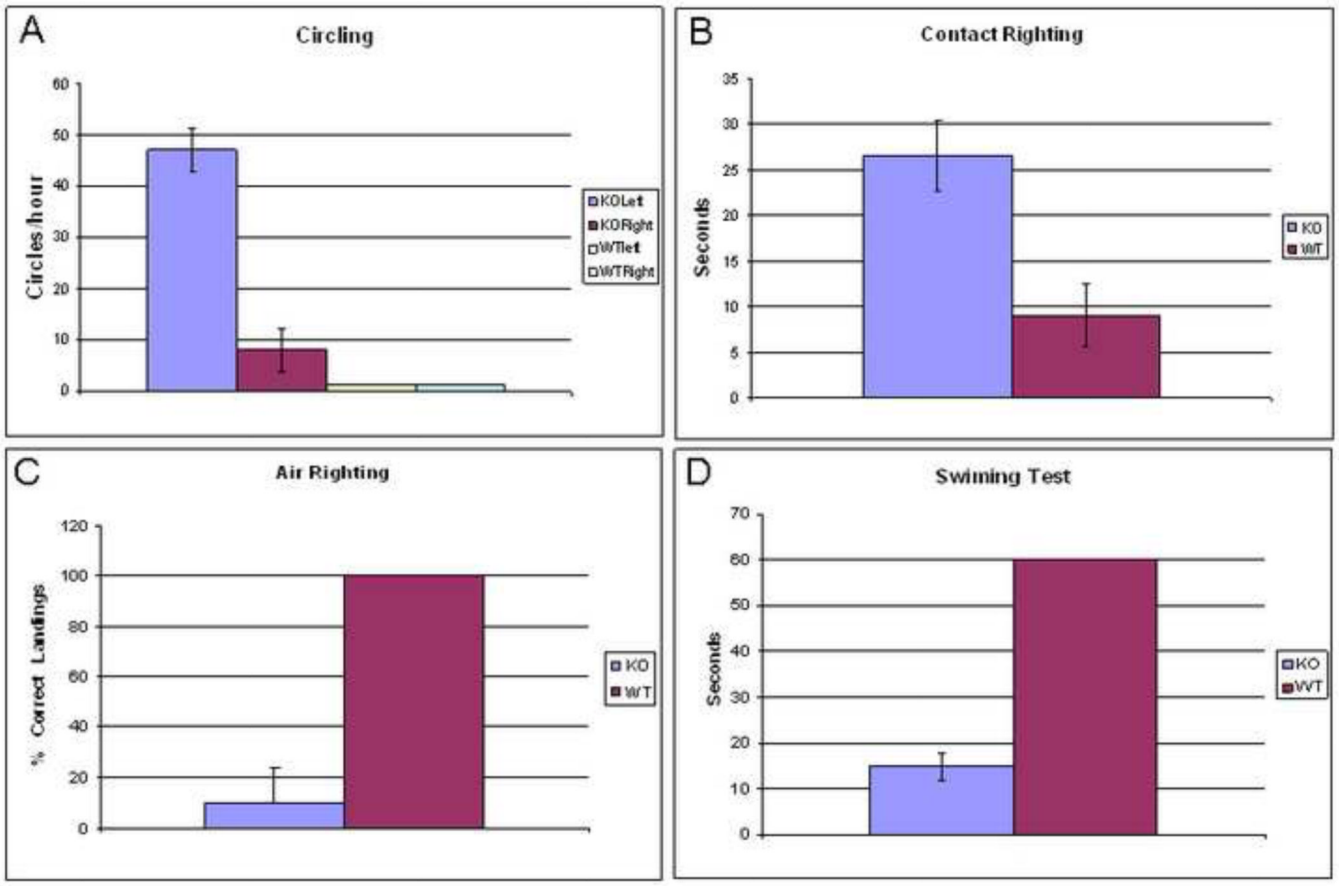

Figure 4.

The vestibular function tests reflect the mean ± S.E.M. for 6 prosaposin KO and 6 wild mice. 4A-The *circling frequency test* quantifies the number of circles occurring in 1 min, showed that WT mice had essentially no circling tendencies, while the KO mice circled, predominantly to the left, though occasionally to the right. 4B-The *contact righting reflex testing* demonstrated that wild-type mice recognized their upside down position and righted themselves inside a large syringe much more quickly than KO mice (WT=10sec vs KO=27sec). Further, KO mice made little or no effort to right themselves. 4C- *Air righting reflex testing* showed that wild-type mice righted themselves in mid-air, landing on their feet 100% of the time while KO mice landed on their back or side 90% of the time. 4D- The *swim test* demonstrated that all WT mice exhibited a normal swimming while not one KO mouse was able to swim or orient properly in water. Taken together, these results show a significant loss of balance in the prosaposin KO mice.

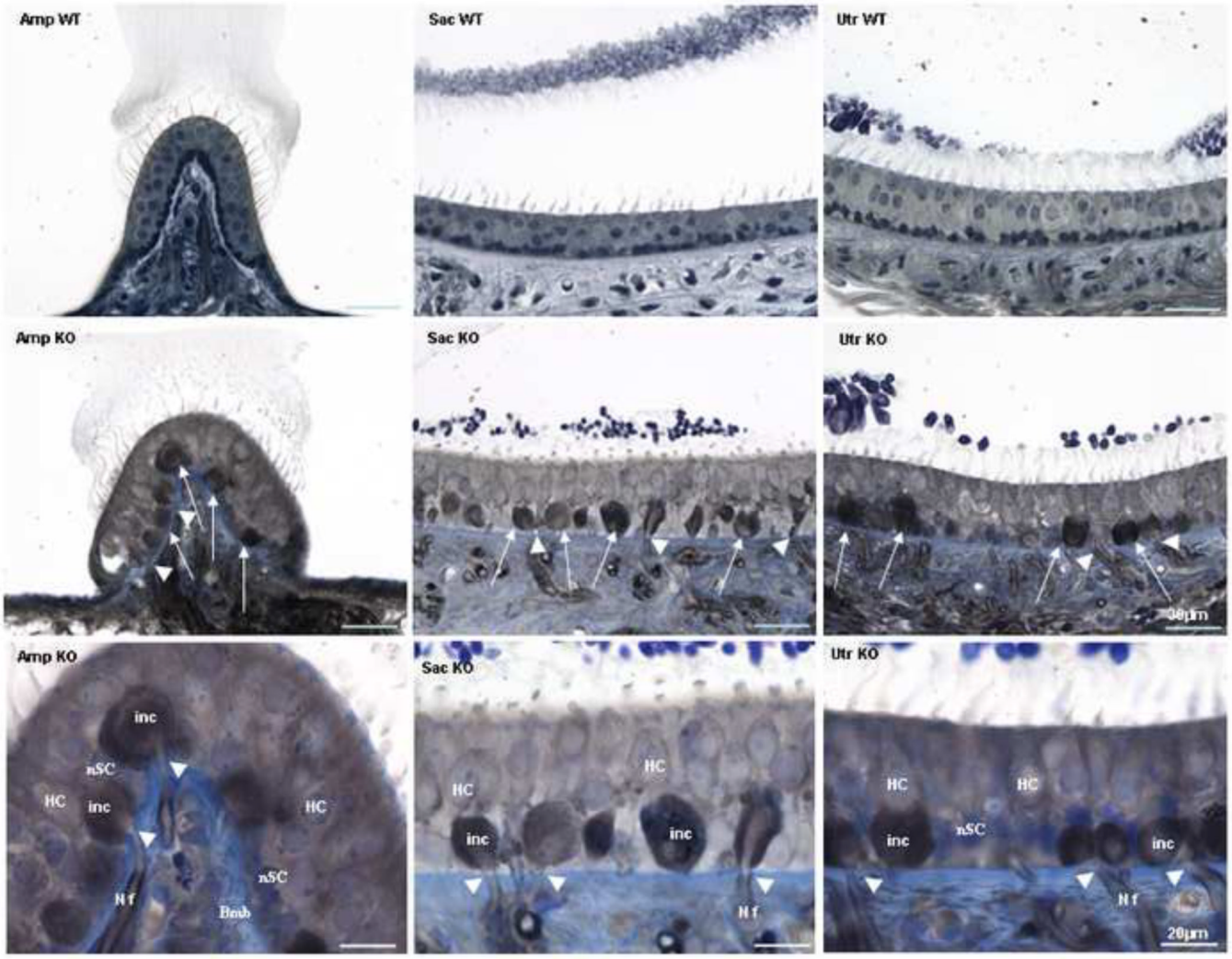

Figure 5.

Light microscopy, toluidine blue-stained sections of the Ampulla (**Amp**), Saccule (**Sac**) and Utricle (**Utr**) from P25 knockout (KO) mice; wild-type (WT) sections are included for comparison. This figure demonstrates that the gross morphology of the vestibular system of the prosaposin KO and WT mice is identical. However, in the KO mice there is exuberant cellular proliferation and vacuolization below the vestibular hair cells. This causes disruption of the supporting cells in all 3 end-organs (arrows) and appears as if some of the afferents entering the epithelium swell upon their entrance beneath the hair cells (arrow heads). The morphology of Scarpa's ganglion was identical in the wild-type and KO mice (data not shown). Scale bars: 30µm.

Last panel shows high magnification (scale bars: 20µm) of the afferents entering the epithelium (NF) swell up (inc: inclusion) as soon as they enter the epithelium right under the hair cells (arrow head). Basement membrane (Bmb), supporting cells nucleus (nSC), hair cells (HC)

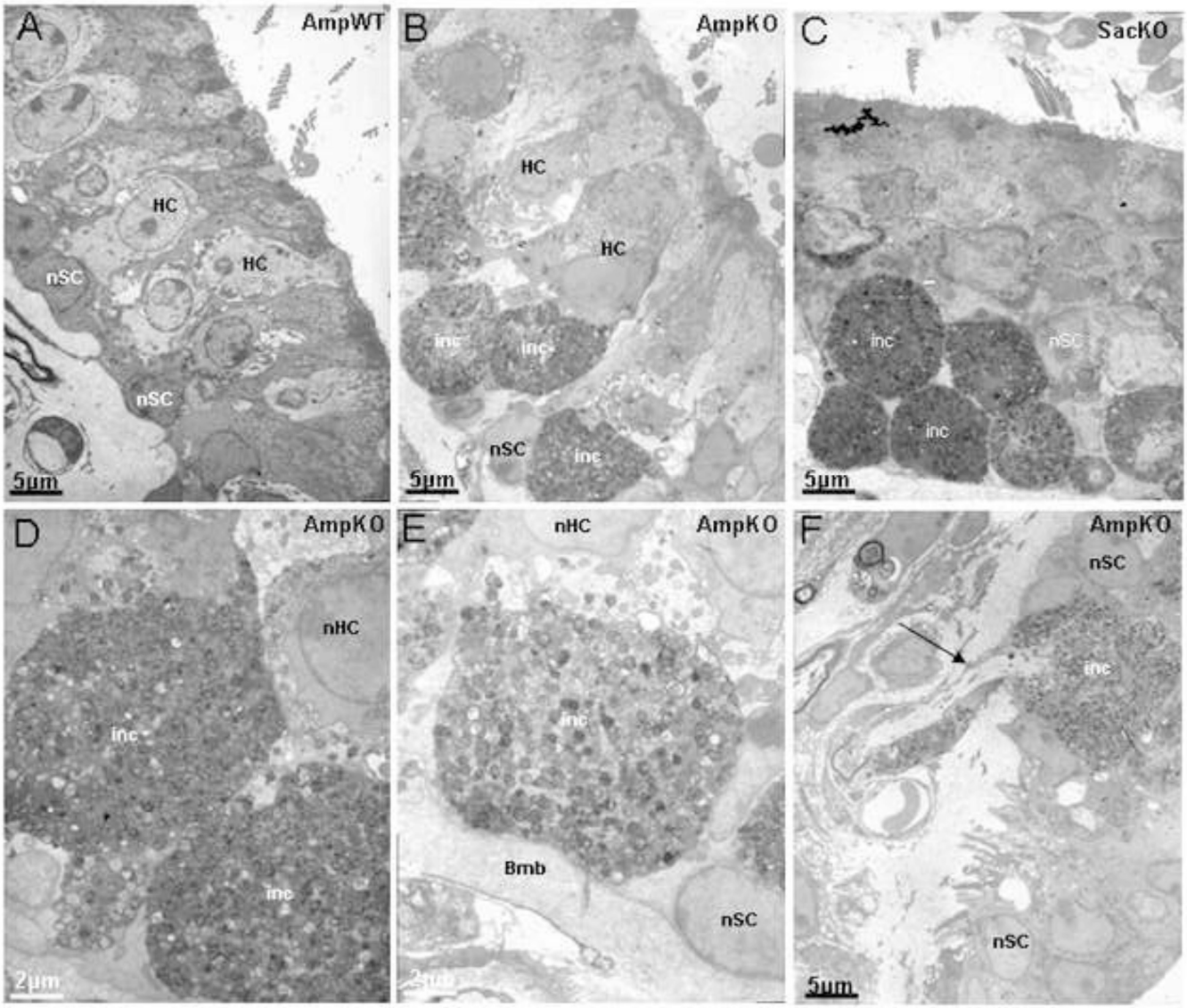

Figure 6.

Electron microscopy of the vestibular epithelium of the prosaposin mice. Low magnification of the Ampulla (**Amp**), Saccule (**Sac**), from a P25 wild (**A**), and KO mice (**B, C** and **F**) Scale bars: 5µm and higher magnification of KO Ampulla (**D** and **E**) Scale bars: 2µm. In contrast to the wild-type, the KO mice demonstrate disruption of the normal organization of the hair cells and supporting cells, including vacuolization and cellular hypertrophy (**B**, **C**, **D**, **E**, and **F**). At higher magnification of KO ampulla (**D** and **E**), the cellular proliferation at the base of the hair cells is striking, with resultant damage to hair cells (HC) and supporting cells (SC) normal structure. The regions of cellular hypertrophy show the granularity of the inclusions (inc). Figure **F** shows that some of the afferents entering the epithelium swell up as soon as they enter the epithelium right under the hair cells (arrow). Basement membrane (Bmb), supporting cells nucleus (nSC), hair cells nucleus (nHC)

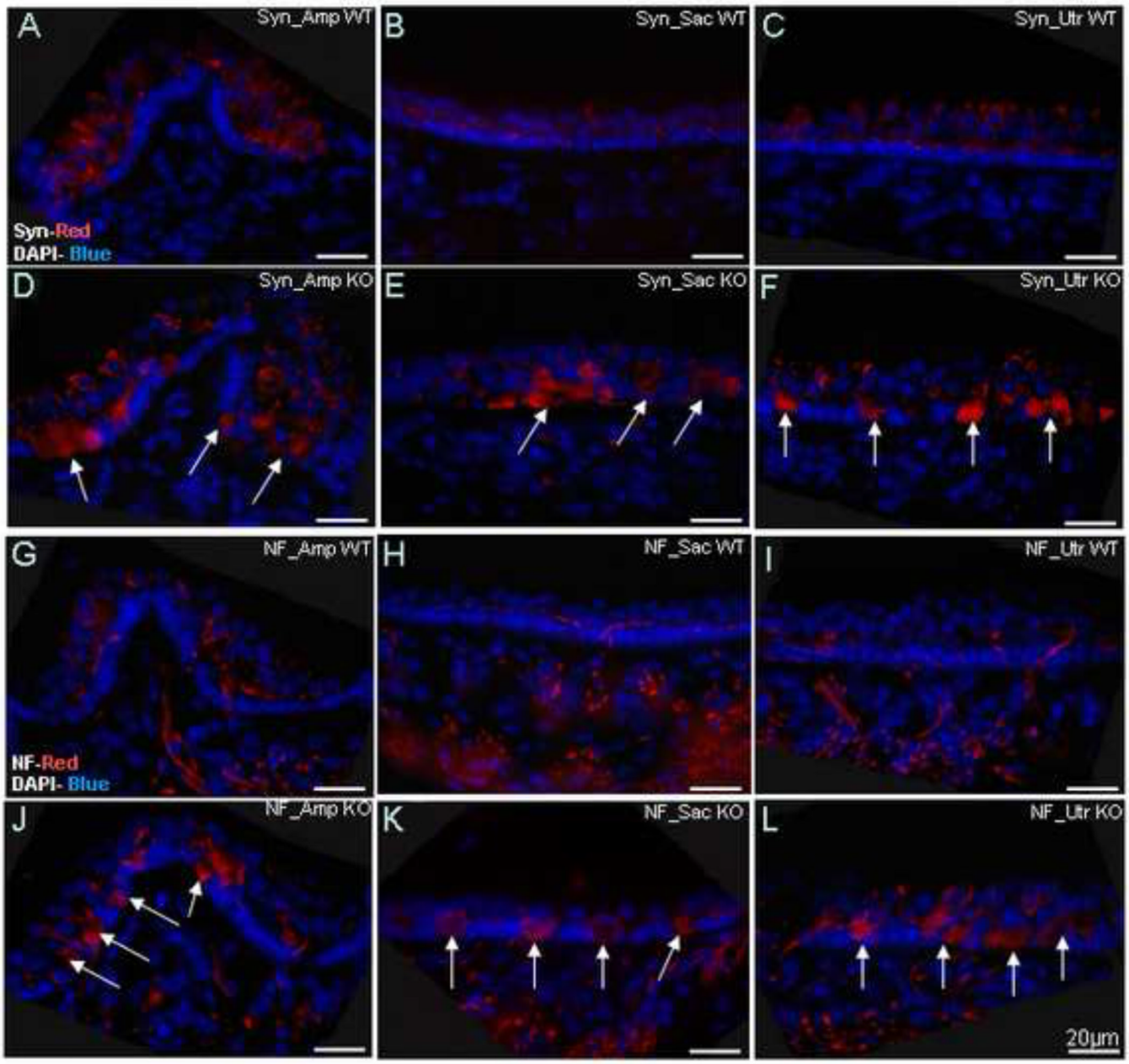

Figure 7.

Synaptophysin (Syn) and neurofilament (NF) staining in the prosaposin WT (A–C for Syn and G–I for NF) and KO (D–F for Syn and J–L for NF) mice. As expected, WT mice demonstrate normal synaptophysin and neurofilament staining patterns (Red), with weak label in the regions of the vestibular hair cells. In contrast, KO mice demonstrate a significant amount of signal of both synaptophysin and neurofilament in the regions precisely corresponding to the cellular proliferation seen in light (figure 5) and electron (figure 6) microscopy. This is seen in all 3 end-organs. Together, these studies demonstrate that the cellular hypertrophy seen is composed of proliferating afferent and efferent neuronal endings. DAPI staining (Blue) was used to counterstain nuclei. Scale bars: 20µm

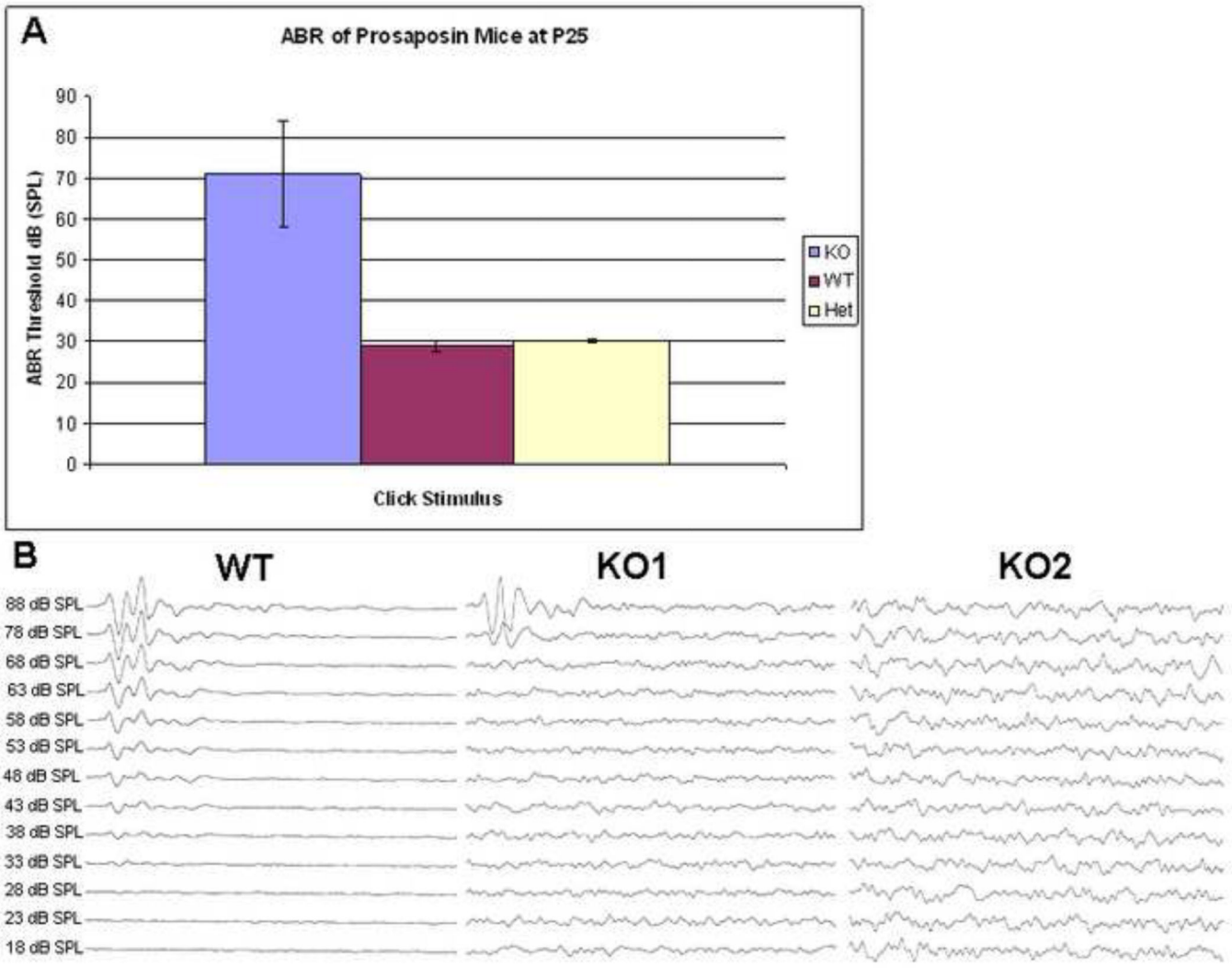

Figure 8.

Auditory brainstem responses (ABR) of the prosaposin mice: ABR thresholds for the prosaposin KO, WT and Heterozygote mice at P25 using a click stimulus (Figure 8A). Results demonstrate statistically significantly higher thresholds in the KO as compared with heterozygote and WT mice. Figure 8B shows the individual ABR wavefoms of the WT as well as 2 KO (KO1 and KO2) mice that have elevated ABR thresholds when compared to the WT.